Oncogene (1999) 18, 4211–4223

http://www.stockton-press.co.uk/onc

Telomere dynamics, end-to-end fusions and telomerase activation during the human fibroblast immortalization process

Caroline Ducray[1], Jean-Patrick Pommier[1], Luis Martins[1], François D Boussin[2] and Laure Sabatier*,[1]

[1]*CEA, DSV/DRR/Laboratoire de Radiobiologie et Oncologie BP6, 92 265 Fontenay-aux-Roses, France;*
[2]*CEA, DSV/DRR/Laboratoire de RadioPathologie BP6, 92 265 Fontenay-aux-Roses, France*

Loss of telomeric repeats during cell proliferation could play a role in senescence. It has been generally assumed that activation of telomerase prevents further telomere shortening and is essential for cell immortalization. In this study, we performed a detailed cytogenetic and molecular characterization of four SV40 transformed human fibroblastic cell lines by regularly monitoring the size distribution of terminal restriction fragments, telomerase activity and the associated chromosomal instability throughout immortalization. The mean TRF lengths progressively decreased in pre-crisis cells during the lifespan of the cultures. At crisis, telomeres reached a critical size, different among the cell lines, contributing to the peak of dicentric chromosomes, which resulted mostly from telomeric associations. We observed a direct correlation between short telomere length at crisis and chromosomal instability. In two immortal cell lines, although telomerase was detected, mean telomere length still continued to decrease whereas the number of dicentric chromosomes associated was stabilized. Thus telomerase could protect specifically telomeres which have reached a critical size against end-to-end dicentrics, while long telomeres continue to decrease, although at a slower rate as before crisis. This suggests a balance between elongation by telomerase and telomere shortening, towards a stabilized 'optimal' length.

Keywords: telomere; chromosomal instability; telomerase

Introduction

Telomeres are the specialized nucleoprotein complexes located at the ends of eukaryotic chromosomes. The structure and the sequence of the telomeres are highly conserved among eukaryotes. The telomeric DNA sequences differ from internal DNA sequences in their primary sequence and their functional properties. The DNA component of human telomeres consists of a G rich strand, running to the 3′ end of the chromosome, composed of a variable amount of simple tandemly repeated sequences (TTAGGG)n. Telomeres serve as a protection against essential genetic information loss since a conventional unidirectional DNA polymerase is unable to completely replicate the very ends of linear DNA, losing telomeric DNA sequences at each round of semi-conservative DNA replication (Watson, 1972; Olovnikov, 1973; Lingner *et al*., 1995). Telomeric sequences lost during synthesis of the lagging strand can simply be restored by *de novo* addition of G-rich repeats to the 3′ end of the chromosome by a specialized ribonucleoprotein complex with a reverse transcriptase activity, called telomerase (Greider and Blackburn, 1985, 1987). Telomerase activity is not detectable in the large majority of somatic cells whereas germinal cells, stem cells and cancer cells present telomerase activity. The telomerase holoenzyme is composed of both RNA and protein subunits. The RNA component provides the template for telomere repeat synthesis. The recent identification of genes encoding human telomerase protein subunits, such as the human catalytic subunit TERT (Meyerson *et al*., 1997; Nakayama *et al*., 1998), has enabled a direct examination of the role of these proteins in the maintenance of telomeres in human immortal cells and their contribution to telomerase activity, the TERT upregulation during immortalization process having been demonstrated.

The presence of telomeric DNA at the chromosomal termini is essential for chromosomal stability. Indeed telomeres are thought to maintain the chromosome integrity during the cell cycle by allowing a proper segregation during cell division. Broken chromosomes that are uncapped become hotspots for different types of recombination (non reciprocal, homologous or illegitimate). They may therefore undergo aberrant recombination, end-to-end fusions and bridge-fusion-breakage mechanisms. Being unprotected, the chromosomes are also susceptible to exonucleolytic degradation (McClintock, 1939; Sandell and Zakian, 1993). Telomeres would also prevent the activation of DNA-damage check-points (Filatov *et al*., 1998). Thus, without these essential structures, the chromosome is unstable.

Normal human somatic cells do not express telomerase activity and have a limited replicative lifespan *in vitro* (Hayflick and Moorhead, 1961; Harley, 1991). The introduction of telomerase in normal diploid cells, expressing the ARN component of telomerase hTERC, maintain normal growth controls, normal karyotypes but present an extended lifespan (Bodnar *et al*., 1998). According to the telomere hypothesis, this finite proliferative capacity would correlate with telomere length: cells with long telomeres can undergo more rounds of cell division *in vitro* than those with short telomeres (Allsopp *et al*., 1992). Telomerase being inactive in somatic cells, the gradual loss of telomeric DNA with each round of replication could eventually lead to chromosomal instability which would contribute to replicative

*Correspondence: L Sabatier
Received 8 November 1998; revised 12 February 1999; accepted 5 March 1999

cellular senescence (Greider, 1991). This finding corroborates the observations of telomeric fusions detected in senescent fibroblasts (Benn, 1976). Cell senescence can be overcome in part by virus induced transformation (Klingelhutz *et al*., 1994). Viral oncogenes will lead to additional mean population doublings beyond the normal cellular senescence checkpoint, which would result in an extended lifespan at the cellular level. This hypothesis was reinforced by the observation of a continued loss of telomere sequences in the transfected cells (Shay *et al*., 1991). Cells presenting critically short telomeres would cease to divide and enter crisis. At this point, chromosomal instability is maximal and characterized by a high amount of telomeric fusions. Although most cells die at crisis, the rare cells that emerge are generally aneuploid, express telomerase activity, and have a stable telomere length (Counter, 1994). Therefore telomerase activation may be a critical step in cell immortalization (Counter *et al*., 1992). Recent results show that although the ectopic expression of telomerase in human somatic cells is sufficient for immortalization, it does not seem to induce changes associated with malignant transformation (Jiang *et al*., 1999; Morales *et al*., 1999).

Telomeric DNA presents a special chromatin structure and is packaged with telomere specific proteins which play a role in chromosome stabilization (Tommerup *et al*., 1994). Telomere structural proteins bind non-covalently and package the single-stranded and double-stranded regions of eukaryotic telomeres. Telomere binding proteins have been identified and characterized in several organisms including vertebrates. Telomere binding protein TRF1 was shown to be involved in telomere length regulation, presumably by regulating access of telomerase negatively (Bilaud *et al*., 1997; Broccoli *et al*., 1997; Shen *et al*., 1997; van Steensel and de Lange, 1997). Moreover, human TRF proteins, released from shortened telomeres, could be involved in signaling cell cycle exit. New evidence has shown a protective role of TRF2 against end-to-end fusions of chromosome ends by maintaining the correct structure at telomeres (van Steensel *et al*., 1998).

We established transformed cell lines from single transfected cells in order to examine the role of telomerase in telomere maintenance in relation to chromosomal instability. We performed a sequential analysis during the immortalization process. Primary cells lose telomeric repeats as the number of divisions increases since they present undetectable telomerase activity. 'Immortalized' transformed cells, which have undergone crisis and reactivated telomerase, still show a decrease in telomere length for several passages with a correlated decrease of chromosomal instability.

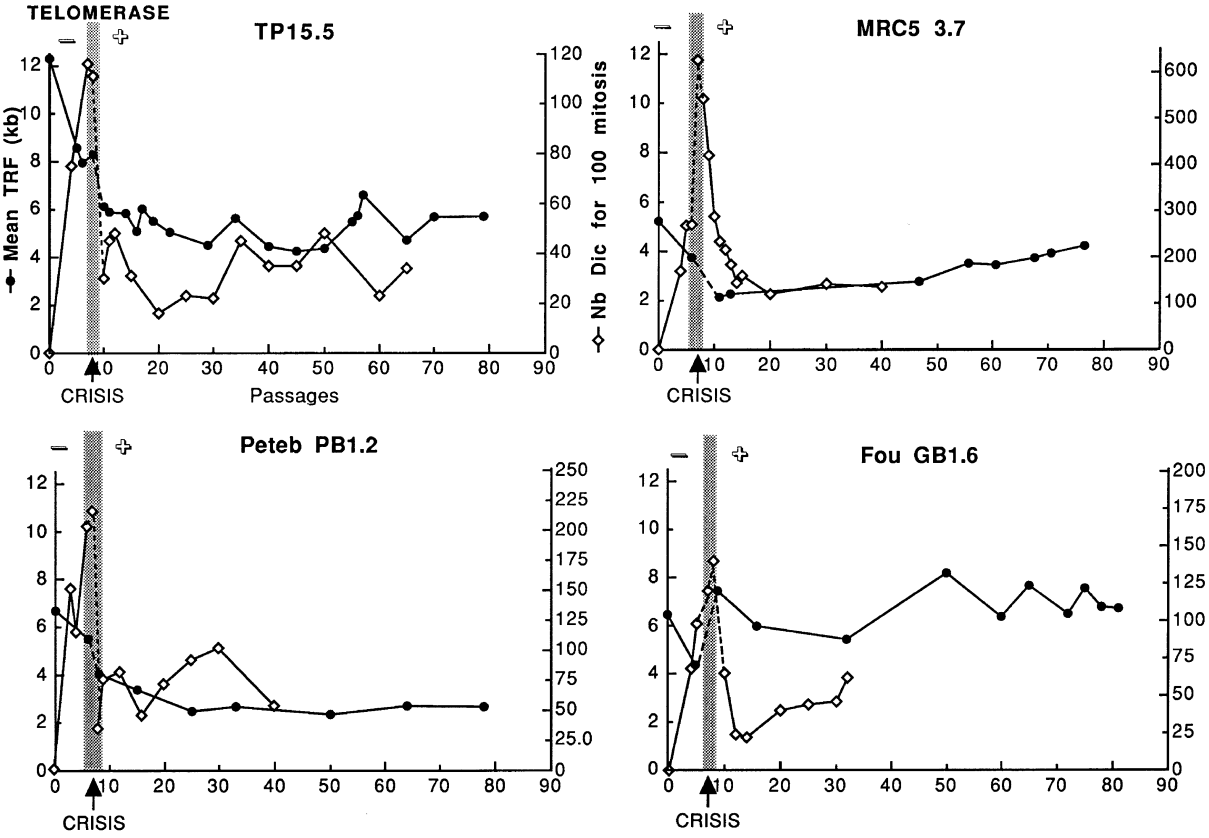

Figure 1 Mean TRF lengths, telomerase activity and chromosomal instability throughout cell proliferation in long-term cultures of four SV40 transformed fibroblast cell lines (TP15.5, MRC5 3.7, Peteb PB1.2 and Fou GB1.6). Mean TRF length analysis (●) was performed from two or three independant Southern blots for each cell line. Passage 0 referred to the time at which normal fibroblasts were transfected with SV40. Telomerase activity is referred to as − (no telomerase activity before crisis) and + (telomerase activity detected after crisis). Telomerase activity tests were performed before and after crisis in six different passages for MRC5 3.7, 7 for Fou GB1.6, 8 for Peteb PB1.2 and 13 for TP15.5. The number of dicentrics in 100 metaphases (◇), representing the chromosomal instability, were estimated from an analysis of 50–100 metaphase spreads stained with giemsa. Their values were significantly different from one cell line to another. In all cases, the maximum was reached during crisis. Cells emerged from crisis at passage 10 for TP15.5, passage 8 for Peteb PB1.2 and passage 9 for MRC5 3.7 and Fou GB1.6

Telomerase activation would result in the protection of telomeric ends without lengthening them unless they have reached a critical threshold.

Results

Telomere length, telomerase activity and chromosomal instability in SV40-transformed fibroblasts

In this study, we used four human fibroblast cell lines transfected by SV40 virus, with each cell line established from a different donor.

Mean TRF

To investigate the effect of cell division on telomeric DNA, we regularly determined the size distribution of the terminal restriction fragments (TRF) composed of telomeric and subtelomeric arrays. Mean TRF lengths for the different fibroblast cell lines are plotted in Figure 1 versus number of passages. TRF lengths in all cell lines decreased gradually with cell proliferation *in vitro* until crisis. After crisis, we observed an evolution of telomere lengths with first an additional telomere decrease, followed by an overall stabilization occurring at different time points after crisis for the different cell lines, with some oscillations in the case of TP15.5 and Fou GB1.6. The minimal mean TRF length reached before stabilization vary among the cell lines: 4.5 kb (TP15.5 passage 29), 3.1 kb (Peteb PB1.2 passage 25), 2 kb (MRC5 3.7 passage 11) and 6 kb (Fou GB 1.6 passage 16). For TP15.5 and Peteb PB1.2 the shortest telomere lengths are not reached during crisis but several passages later. Thus telomere erosion continues after crisis in these two cell lines. The 'stabilized' telomere length in immortal cells is shorter than in normal parental cells, except for Fou GB1.6 where there is no significant difference.

This post-crisis telomere attrition observed in two out of the four cell lines studied is reinforced when we take into account the heterogeneity of the telomere lengths which is poorly reflected by mean TRFs. Indeed these cell lines present a special pattern of TRFs on Southern blots. The TRFs of TP15.5 and Peteb PB1.2 immortalized cell lines are composed of several populations of telomere lengths as shown in Figure 2. Both high and low telomeres decrease in size after crisis. Homogeneization of telomere lengths is observed after passage 29 for TP15.5 and after passage 25 for Peteb PB1.2.

Telomerase activity and expression of telomerase subunits

To establish the temporal pattern of telomerase expression during transformation and immortalization, we assayed for enzyme activity in these four fibroblastic cell lines before and after crisis using two tests for most samples, TRAPeze (Appligene, Illkirch) and TRAP-ELISA (Boehringer-Mannheim, Meylan) (Figure 3). Telomerase activity was undetectable in pre-crisis SV40-transformed cells but was expressed in post-crisis immortalized cells as soon as the cells emerged from crisis, in the four cell lines. In the TP15.5 cell line, telomerase activity appeared strongly right after crisis emergence followed by a decrease a few passages lateron but increased thereafter. Although

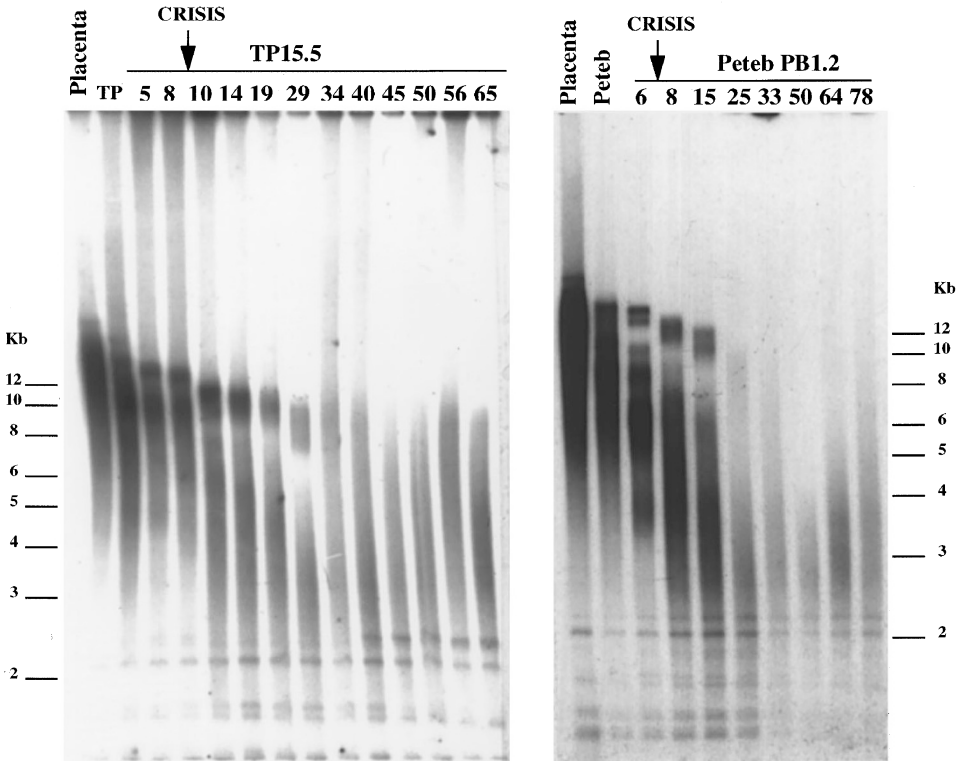

Figure 2 TRF length in SV40 transformed fibroblast cell lines TP15.5 and Peteb PB1.2. Southern hybridizations of the telomeric probe $(TTAGGG)_4$ on 0.5% agarose gels to *Rsa*I-*Hinf*I-digested DNA at the indicated passages shows the presence of several subpopulations of TRFs in these two cell lines. TP and Peteb refer to normal fibroblasts at the time of transformation with SV40

telomerase activity is detectable *in vitro*, telomeres still continue to decrease (Figure 1). In order to study telomerase activation during the progression in culture of the TP15.5 cell line, the expression of TERC, TERT (RNA and catalytic subunits of telomerase respectively) and TEP1 (protein associated to telomerase activity) was analysed. The results of the Northern blot showed a detectable expression of TERC throughout the culture before as well as after crisis (Figure 4a). In passage 7 its expression was rather moderate, with a peak at passage 13, whereas from passage 21 on, TERC mRNA signal intensity did not seem to vary (Figure 4b). This suggested that telomerase activity was not regulated on its RNA component basis after immortalization as it has been previously described (Feng *et al*., 1995; Blasco *et al*., 1996). The variations of expression of TERT and TEP1 was studied by RT-PCR (Figure 5a). The expression of TERT is undetectable before crisis and appears after crisis. This result is in agreement with the detected telomerase activity (Harrington *et al*., 1997; Meyerson *et al*., 1997; Nakayama *et al*., 1998). As for TERC our results showed that the expression pattern of the telomerase associated protein TEP1 is widespread, present in normal fibroblasts, precrisis and post-crisis fibroblasts, even when telomerase activity is not detectable.

Chromosomal instability

A dramatic increase in the number of dicentric chromosomes reaching its peak during the crisis period was observed in all the cell lines. This increased chromosomal instability was associated with a progressive loss of telomeric DNA in pre-crisis cells (Figure 1). We observed a direct correlation between

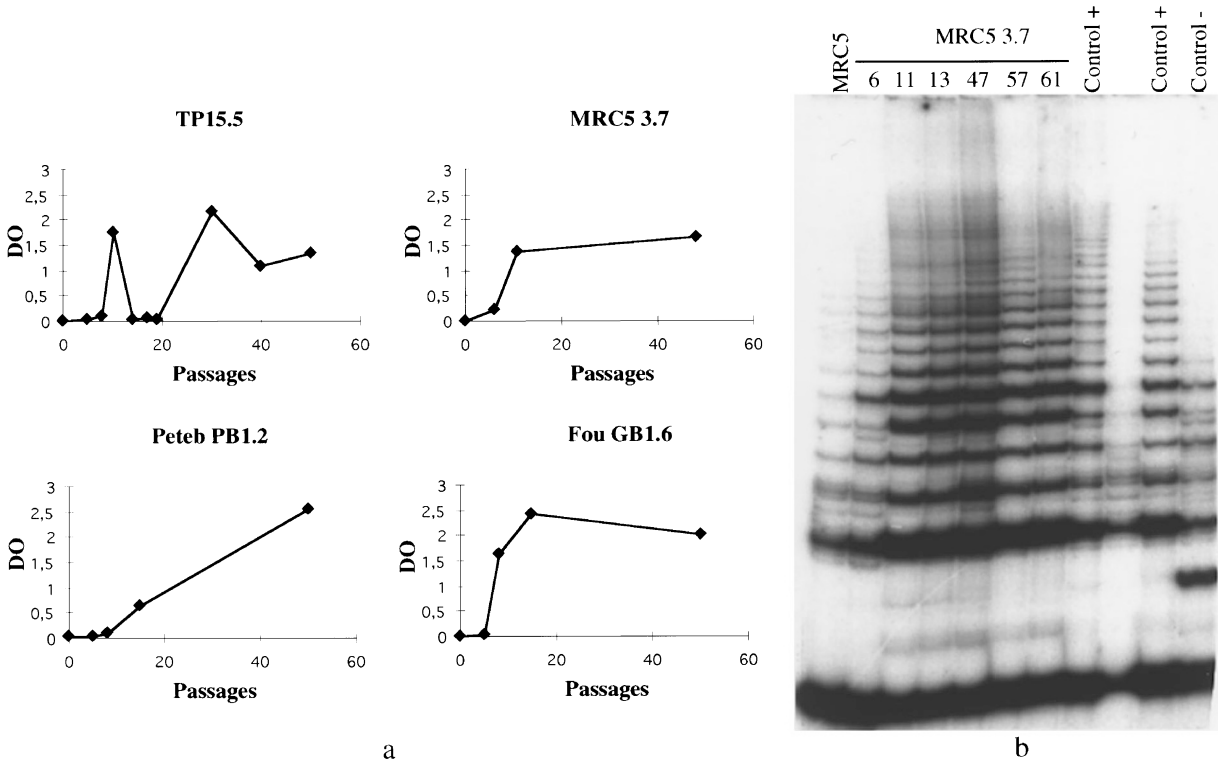

Figure 3 Telomerase activity observed in (**a**) by TRAP ELISA in all four cell lines and in (**b**) by TRAPeze in the MRC5 3.7 cell line. For TP15.5, triplicates were carried out giving standard deviation values enclosed around 0.18. In the TRAPeze experiment, the negative control refers to an RNase control

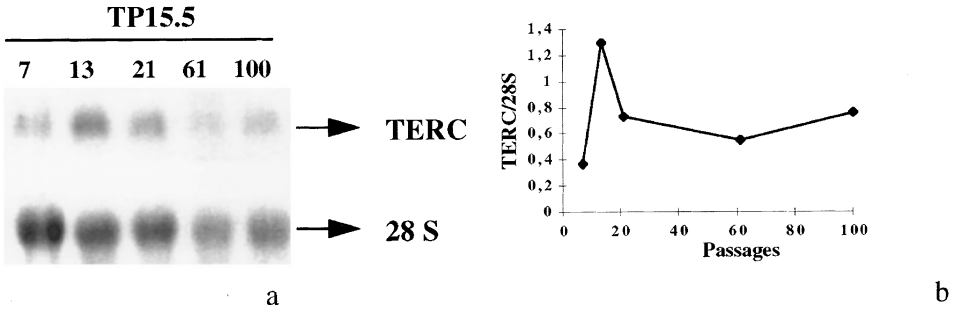

Figure 4 (**a**) mRNA expression of human telomerase RNA component, TERC. Northern hybridization of TERC on a 1% agarose gel and control 28S on the same filter after dehybridization. (**b**) Representation of the ratio between TERC and 28S intensities for each analysed passage

short telomere length measured in the first passage after crisis and the maximal value of chromosomal instability except for Fou GB1.6 which presents an increase in telomere length during crisis. Indeed we scored 116 dicentrics for TP15.5 (mean TRF: 6.1 kb, passage 10), 140 dicentrics for Fou GB 1.6 (mean TRF: 7.4 kb, passage 9), 216 dicentrics for Peteb PB1.2 (mean TRF: 4.3 kb, passage 9) and 626 dicentrics for MRC5 3.7 (mean TRF: 2.1 kb, passage 11) in 100 metaphases analysed. The evolution of dicentrics as a function of mean TRFs indicates an inverse correlation, with correlation coefficient R^2 enclosed between

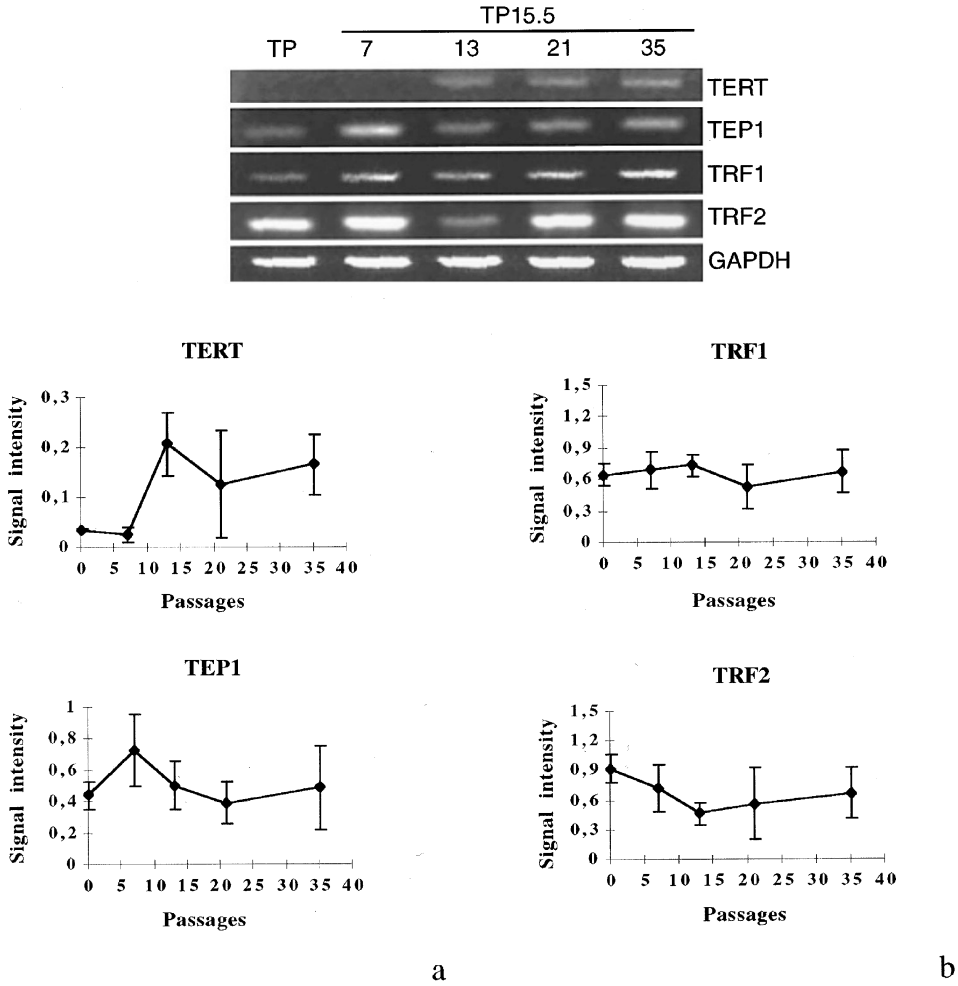

Figure 5 mRNA expression studied by RT–PCR. Each point corresponds to the ratio of mean value of triplicates of the studied mRNA over that of GAPDH. (**a**) mRNA expression of human telomerase components (TERT and TEP1) during proliferation of TP15.5 in culture. (**b**) mRNA expression of human telomere binding proteins (TRF1 and TRF2) during proliferation of TP15.5 in culture

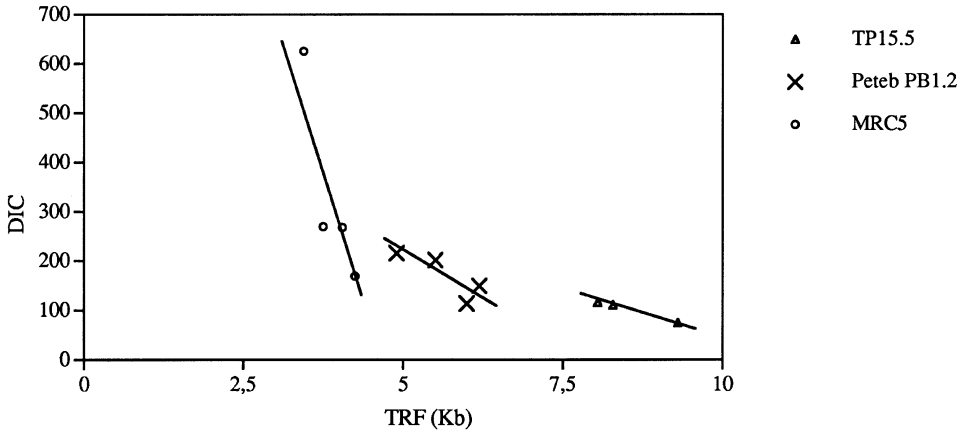

Figure 6 Correlation between mean TRF and dicentric frequency before crisis. TRF refers to the mean TRF length and DIC represents the number of dicentrics in 100 metaphases. The correlation coefficient R^2 value is 0.9951 for TP15.5, 0.7225 for Peteb PB1.2 and 0.8126 for MRC5 3.7

0.72 for Peteb PB1.2 and 0.99 for TP15.5 (Figure 6). The compilation of the three cell lines (TP15.5, Peteb PB1.2 and MRC5 3.7) suggests a strict correlation between telomere length and chromosomal instability before crisis obeying an exponential evolution ($R^2 = 0.8572$) in the occurrence of chromosomal instability. A dramatic increase in the number of dicentrics is induced for mean TRF values below 4 kb which could indicate a 'critical size' in telomere length. After crisis, chromosomal instability drops drastically and remains rather low although mean telomere length still decreases in two cell lines (Figure 1).

Chromosome regions involved in dicentrics

In order to characterize the sporadic chromosomal instability before and after crisis, we monitored breakpoint locations in dicentrics throughout *in vitro* proliferation by R-banding labeling of TP15.5 metaphases (Table 1). As expected the number of terminal-terminal fusions is very high at passage 7, just before crisis, where most of the cells die (Counter *et al*., 1992). We scored the number of chromosome breaks, occurring in telomeres, euchromatine and centromeres, in order to calculate the implication of the different chromosome regions in the metaphases displaying at least one dicentrics. Among these metaphases analysed for each chosen passage, the percentages of telomeric, euchromatic and centromeric involvements in the non-clonal dicentrics were calculated and compared to theoretical values on the basis of telomeres and centromeres representing 23% and 12.5% of the genome respectively considering the bias inherent to the cytogenetic analysis. In all passages studied, the percentage of breakpoints located at telomeres was significantly higher than that occurring in euchromatin and centromeres affected in the formation of dicentrics (Chi(2) test). Therefore, whether before or after crisis, telomeres were the chromosome structures systematically over-involved in the breakpoints of the dicentrics analysed. During crisis, 84.3% of the breakpoints involved in dicentrics are telomeric versus 62.5% after crisis. Thus the majority of the dicentrics formed were of telomeric origin, ruling out the possibility that the high amount of dicentrics observed during crisis was due to the over-involvement of other chromosome structures than telomeres. Thus the chromosomal instability observed is of the same nature before, during and after crisis.

Table 1 Localization of chromosome breakpoints during proliferation of TP15.5 in culture

Passage	*Nb of breaks/ Nb of mitoses analysed*	*Telomeres (%)*		*Euchromatin (%)*	*Centromere (%)*	
4	38/14	73.7	+	15.8	10.5	=
7	108/30	84.3	+	9.3	6.4	=
10	16/10	62.5	+	6.2	36.3	=
11	22/14	72.8	+	13.6	13.6	=
12	34/16	61.8	+	2.9	35.3	=
20	10/10	50	+	10	40	=
25	8/13	75	+	12.5	12.5	=
30	30/28	76.7	+	3.3	20	=
60	20/10	65	+	10	25	=

The number of breaks occurring in these non-recurrent dicentrics were enumerated in 10 to 30 metaphase spreads. Telomere, euchromatin and centromere implications were scored. A χ^2 test was performed to determine the over-involvement (+) (the probability that the calculated value was equal to the theoretical value was less than 0.05) or expected theoretical involvement (=). Theoretical data was calculated on the basis of telomeres and centromeres representing 23% and 12.5% of the genome respectively, taking into account the cytogenetic bias

Expression of telomere binding proteins

Since telomeric binding proteins have been shown to be involved in telomere end stabilization, we analysed the expression of TRF1 and TRF2 by RT–PCR throughout cell immortalization of TP15.5 (Figure 5b). Their expressions were detectable in all passages analysed without significant variations as the culture progressed up to passage 35.

Bal 31 digestion

We have observed a high percentage of end-to-end dicentrics throughout all passages (Table 1) and a high heterogeneity in TRF lengths for the TP15.5 cell line (Figure 2). We tested the hypothesis of the populations of high TRF lengths in Figure 2 representing interstitial telomeres located in end-to-end fusions. Therefore, we performed the following Bal 31 experiment on TP15.5 postcrisis DNA at passages 14 and 29. In intact DNA, telomeres are preferentially digested by the exonuclease Bal 31. The rate at which Bal 31 removes DNA from the ends increases with time. In the Southern blot

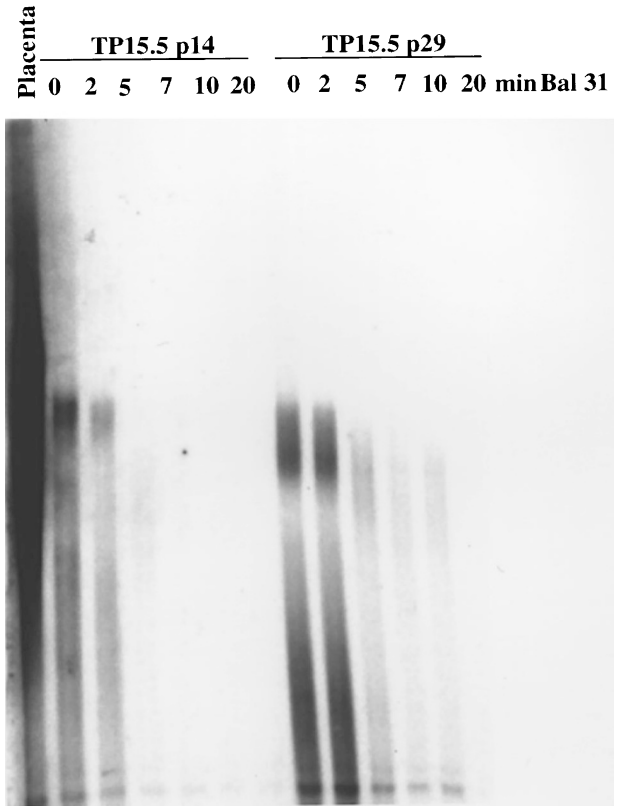

Figure 7 Cinetic study of Bal 31 digestion study on DNA of TP15.5 after crisis, at passages 14 and 29. DNA was digested with *Rsa*I and *Hinf*I after the action of exonuclease Bal 31 for 2, 5, 7, 10 and 20 min

shown in Figure 7, intact TP15.5 DNA was digested for 2, 5, 7, 10 and 20 min and was subsequently cleaved by *Rsa*I-*Hinf*I. This DNA was then analysed with a telomeric probe to measure the rate of Bal 31 digestion and to determine the loss of telomeric repeat signals at each time point. Figure 7 shows that the telomeric fragments shortened rapidly (less than 2 min of Bal 31 digestion) for the populations of low TRFs as well as the populations of high TRFs. Since all populations were affected by Bal 31 digestion, we could rule out the possibility of the high TRF populations actually representing interstitial telomeric tracts. Thus the heterotgeneity of TRFs is due to a large variation in TRF lengths at the very ends of the chromosomes.

Characterization of a homogeneity of the cell population in TP15.5

Having previously shown that TP15.5 presented heterogeneous populations of TRFs, that telomeres are still decreasing after crisis while telomerase activity is detectable and chromosomal instability is low, we decided to address the question of the diversity of the telomere populations by *in situ* cell to cell analysis.

Fluorescence in situ *hybridization of telomere repeats*

In addition to TRF analysis by Southern blotting, we performed fluorescence *in situ* hybridization (FISH) to determine the intensity status of the telomere repeats at chromosome ends on an individual cell level and on a cell population level. Terminal repetitive sequence tracts of TP15.5 were detected with a labeled $(CCCTAA)_3$ peptide nucleic acid probe. The quantification of telomeric signals was carried out after image capture using a CCD camera.

In interphasic cells The interphase FISH method, based on the quantification of the total telomeric fluorescence of each nuclei, shows a Gaussian gathering for all passages studied, whether they presented an homogenized pattern of TRFs (TP15.5 p55) or several TRF populations by Southern blot (TP, TP15.5 p5 and p11). Figure 8 illustrates the distribution of telomeric signals of TP15.5 at passage 11, based on the analysis of one field of 91 nuclei. This Gaussian distribution, also present in the other passages, indicates an homogeneity of telomeric signals between the cells. This strongly suggests that the heterogeneity in TRF lengths observed in TP, TP15.5 p5 and p11 is not due to a mixed population composed of cells with long telomeres and cells with shorter ones.

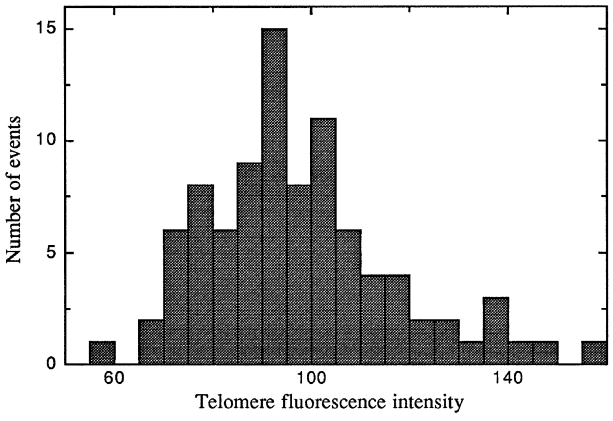

Figure 8 Telomere fluorescence intensity distribution of 91 interphase nuclei of TP15.5 p11

In metaphasic cells We then tested that the TRF heterogeneity was due to intracellular variations in telomere length. By FISH, chromosomes displayed variably intense telomere fluorescence depending on their telomere length. Measured telomere fluorescence intensity values are proportional to the amount of target telomeric sequence (Lansdorp *et al*., 1996). Essentially all chromosomes showed four fluorescent spots at telomeric positions.

Quantification of telomeric signals was performed in ten metaphases of TP, TP15.5 p5, p11 and p55. One of these ten metaphases is shown in Figure 9a. We analysed end-to-end dicentric chromosomes for telomeric sequences at the fusion points. Interestingly, very weak or no telomeric signals were detectable in TP15.5 p7, before crisis, at these locations (Figure 9b), confirming that end-to-end fusions occurred when telomeres are very short and that the populations of high TRFs could not have been composed of interstitial telomeres (consistent with our Bal 31 digestion experiment). Each of these ten analysed metaphases for each passage exhibited the same distribution with slight variations of terminal telomere fluorescence intensities. This, in addition to the absence of intercellular heterogeneity previously shown, allowed us to pool the results of all ten metaphases in the Figure 10. The telomere fluorescence distributions evolved with passages. The distribution was asymmetrical in TP as well as in TP15.5 p5 and p11 (skewness of the distribution >1). Indeed most intensity values, corresponding to short telomeres, were concentrated in the low range while the subset of high intensity values was diffuse. In the same way, in TP, TP15.5 p5 and p11, respectively 3.19, 3.7 and 2% of total telomeres were undetectable, probably because of their too short size. At passage 55 only 0.7% of telomeric signals were undetectable and the scattered high values disappeared. Throughout the passages, telomere intensities underwent modifications leading to a homogeneization observed at passage 55 with a shift of the most represented category of telomeres towards higher intensity values. This was confirmed by the standard deviation analysis which showed an overall decrease of the intracellular heterogeneity of telomere intensities from TP to TP15.5 p55, visualized by the standard deviation mean values represented by the central lines in each box plot (Figure 11).

The differences in telomere length as measured by *in situ* hybridization both in metaphase cells and in interphase nuclei, and Southern blot analysis are therefore comparable. Thus the heterogeneity of TRF lengths shown by Southern blotting represented an intracellular heterogeneity rather than the presence of different cellular populations, each with a different telomere size distribution.

Discussion

In this study, we performed a detailed cytogenetic and molecular characterization of four SV40 transformed cell lines by regularly monitoring the size distribution of terminal restriction fragments, telomerase activity and the associated chromosomal instability. Our experiments showed a correlation between the number of cell divisions, decreased telomere length, the onset of crisis and end-to-end chromosome fusions of telomeric origin consistent with loss of telomeric function confirming that regulation of telomere length is critical for determining the lifespan of individual human cells.

In the four SV40 fibroblastic transformed cell lines studied, emerging post-crisis cells were rare immortalized transformed cells expressing telomerase activity which was undetectable in pre-crisis cells. This is in agreement with the model in which the activation of telomerase expression occurs as a discrete event that permits passage through crisis and cellular immortali-

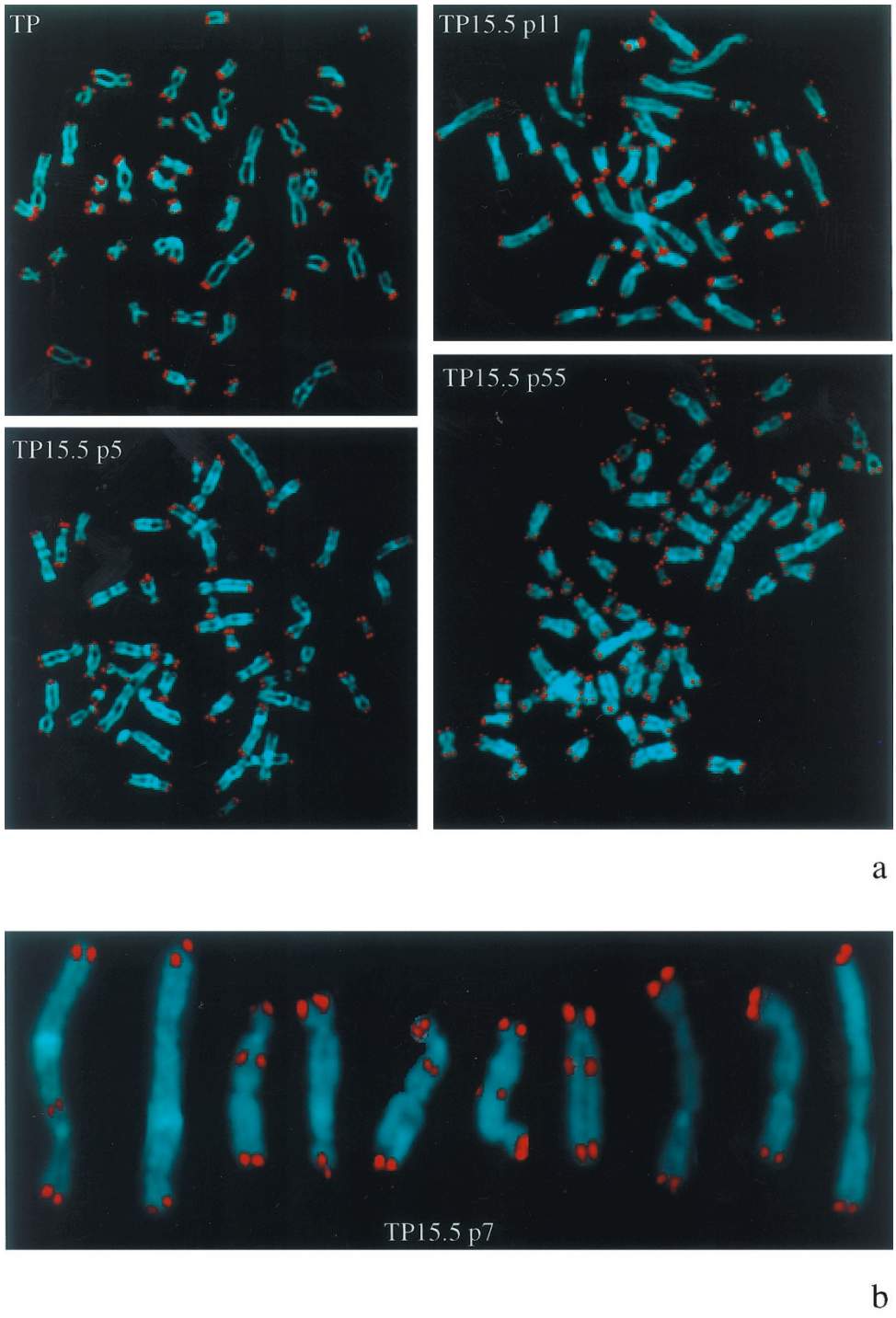

Figure 9 PNA-FISH on metaphasic cells. (**a**) TP, TP15.5 p5, p11 and p55 chromosomes hybridized with the Cy3 PNA $(CCCTAA)_3$ telomeric probe and counterstained with DAPI. (**b**) TP15.5 p7 dicentric chromosomes hybridized with the Cy3 PNA $(CCCTAA)_3$ telomeric probe and counterstained with DAPI. Exposition times were optimized in order to detect eventual interstitial fluorescent signals

zation (Wright *et al*., 1989; Wright and Shay, 1992; Counter, 1994; Rhyu, 1995; Holt *et al*., 1996). Telomerase activation was correlated in TP15.5 with the expression of the catalytic subunit of telomerase TERT, as shown by others (Harrington *et al*., 1997; Meyerson *et al*., 1997; Nakayama *et al*., 1998). The commonly admitted model after immortalization describes a stabilization of telomere lengths as telomerase is activated (Greider, 1991; Counter, 1994; Rubin, 1998). We explored the relationship between telomere length dynamics and telomerase activity after transformation, in the pre-crisis stage, directly after crisis and later on. In the present study, a significant reduction of telomeric length was observed during the extended lifespan of transformed cells until crisis for all cell lines but this also occurred thereafter in two cell lines, TP15.5 and Peteb PB1.2. Thus, the simple model of telomere length stabilization by telomerase activity in transformed cells was not strictly accurate for these two cell lines. Telomerase did not prevent all telomeres from shortening, as previously shown in human thyroid cancer cells (Jones *et al*., 1998).

Indeed analysis of TRF values of TP15.5 and Peteb PB1.2 immortalized cell lines revealed a complex pattern since it demonstrated the heterogeneous nature of the samples. They were composed of a large polymorphism in telomere lengths and distinct TRF populations could be distinguished. All these telomeres seemed to progressively decrease before as well as after crisis. This polymorphism was not due to the presence of interstitial telomeric sequences in TP15.5. This heterogeneity in TRF values observed in Southern blots was demonstrated to result from intracellular heterogeneity in telomere length, by FISH analysis on global cell populations and individual cells. Therefore the decrease of telomere length observed after crisis in spite of telomerase activation is not the consequence of cellular diversities. Thus each cell appears to be composed of a heterogenous distribution of telomere lengths which tends towards a homogeneization. This homogeneization, observed by FISH, occuring a long time after crisis (TP15.5 p55) resulted from a decrease of the long telomeres and an increase of the short telomeres, which could correspond to the telomeres of specific chromosomes. This strongly suggests that telomerase lengthens specifically short telomeres.

Mean telomere length stabilization was observed later on after crisis in TP15.5 and Peteb PB1.2, and right after crisis for MRC5 3.7 and Fou GB1.6. This stabilization can be more complex, as seen in TP15.5 and Fou GB1.6, with oscillations of telomere lengths around an 'optimal' size (Sprung *et al*., 1998). Telomerase could therefore add telomeric repeats on the specific telomeres which have reached a critical short size. This elongation was followed by a rapid shortening which could give rise to the lengthening of telomeres, and so on in a cyclic manner.

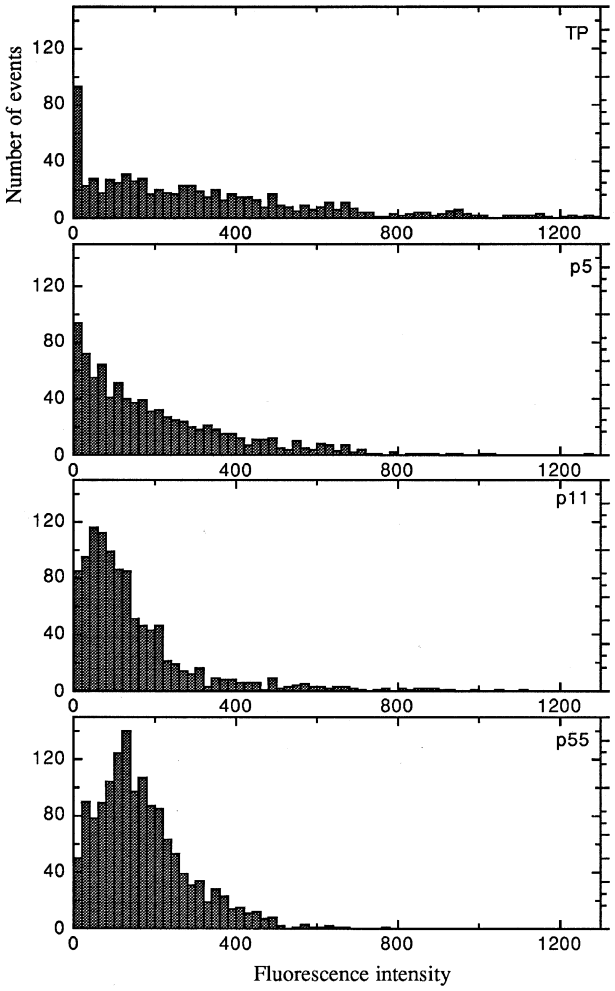

Figure 10 PNA-FISH on metaphasic cells. Distribution of telomere fluorescence intensities in arbitrary units of ten pooled metaphases of TP, TP15.5 p5, p11 and p55, calculated from digital images. In the case of TP some rare intensity values (2%) were observed in a range between 1300 and 3000 but not shown in order to present the same scale for all passages

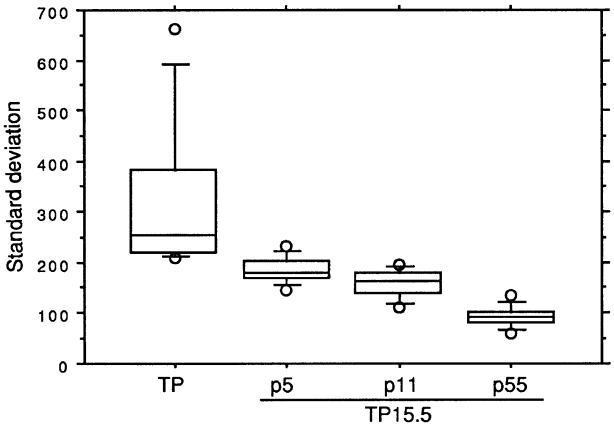

Figure 11 Box plots comparing the distribution of telomere intensity standard deviation values between TP, TP15.5p5, p11 and p55. Each box plot represents the dispersion variability of standard deviation values from ten metaphases for each passage. Each standard deviation value refers to the type of distribution of the fluorescent telomere signals for one metaphase. This dispersion is composed of four parameters: (1) a central line to indicate the median value calculated from the ten standard deviation values. Median values show the evolution of the intracellular dispersion among the different passages analysed; (2) a box to indicate variability around this central tendency between the 25th and 75th percentile (lower and upper limits of the box); (3) whiskers around the box to indicate the 10th and 90th percentile; and (4) circles representing the minimum and maximum standard deviation values. The size of the boxes is proportional to the variability between the ten metaphases of a given passage on the standard deviation basis

Chromosomal instability has been associated with telomere shortening during cellular proliferation *in vitro* (Counter *et al*., 1992; Filatov *et al*., 1998). During the period of crisis the frequency of dicentric chromosomes dramatically increased. Among the four cell lines studied, an inverse relationship was observed at crisis between the mean TRF length and the number of dicentrics. The low detection of telomeric sequences at the fusion points shown by *in situ* hybridization in end-to-end dicentrics observed in cells without telomerase activity (before crisis) reinforces the model in which short telomeres are involved in dicentrics. The low number of telomere repeats occurring in these fusions was also observed in human ovarian epithelial cells (Wan *et al*., 1999). In these studies, we observed the peak of chromosome abnormalities at crisis when telomeres seemed not to be at their shortest length for TP15.5 and Peteb PB1.2. Two hypothesis can be raised concerning the action of telomerase right after crisis leading to a decrease in dicentric rates: (1) telomerase could protect the telomeres against end-to-end dicentrics but without elongating the telomeres which continue to decrease. This hypothesis is reinforced by the lack of detection of telomerase activity few passages after crisis in TP15.5; (2) the protection of chromosome ends could be linked to a balance between the shortening of TRFs and their elongation.

When telomerase activity is detectable, the associated chromosomal instability was relatively weak, however it was always characterized by a majority of end-to-end fusions, suggesting that unstable short telomeres were still present but in small proportion. Thus telomerase which was detected right after crisis could hold a vital role in

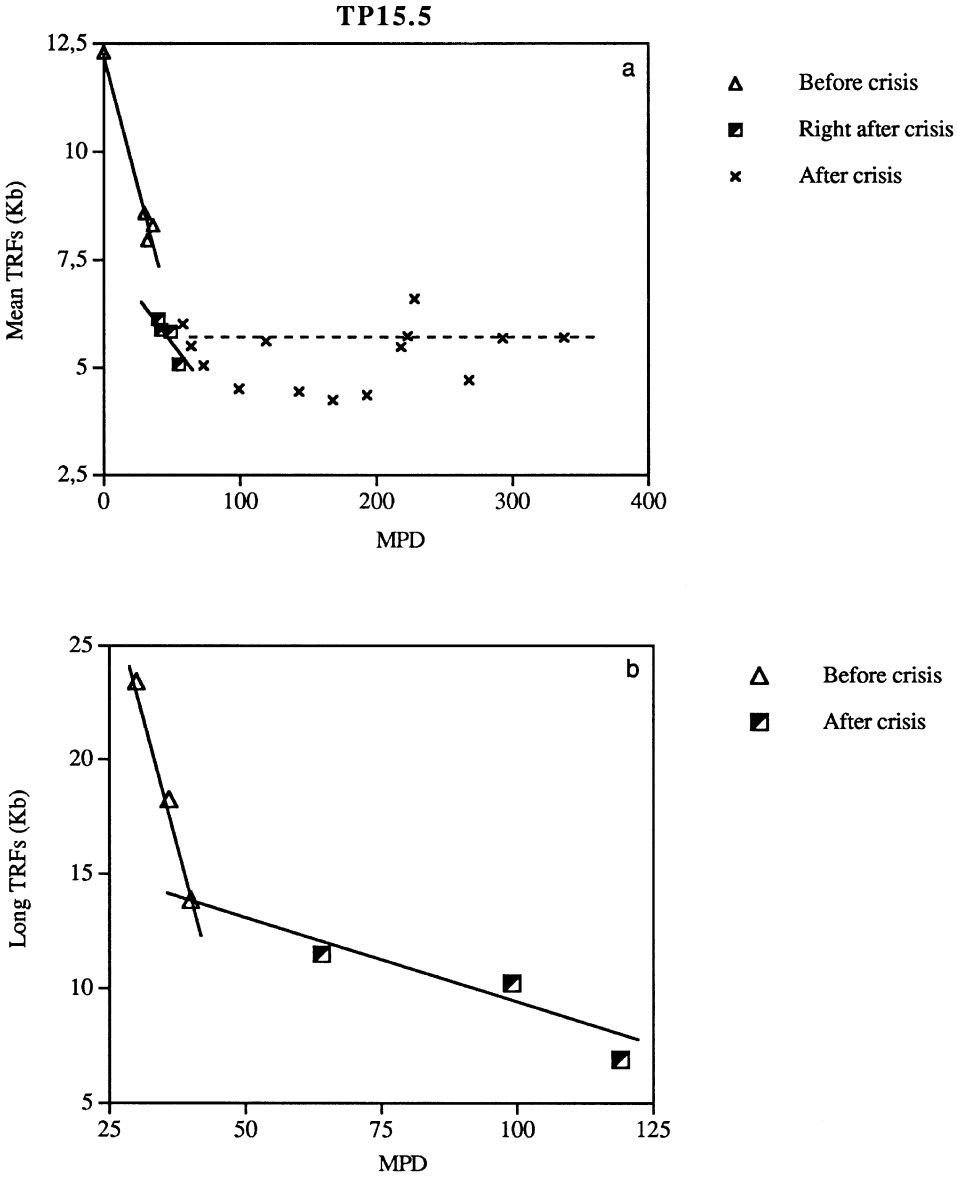

Figure 12 Evolution of TRF length as a function of mean population doublings (MPD) in TP15.5 (**a**) mean TRF, (**b**) TRF from the long telomere population). Different periods were distinguished −before crisis, −right after crisis, −a long time after crisis. The slope of each line was determined: (**a**) −0.12 before crisis, −0.06 just after crisis and 0.0013 during the stabilization of mean TRF lengths; (**b**) −0.95 before crisis and −0.008 after crisis for the long TRFs

restoring telomere function by protecting specifically short telomeres which would otherwise give rise to dicentrics. Therefore cells remain viable with short telomeres provided that they are stably maintained by telomerase. This 'protection' right after crisis could have occurred with or without elongation of the short telomeres. Mean TRFs after crisis (TP15.5, Peteb PB1.2) still decrease until they reach an 'optimal size'. The active role of telomerase in telomere elongation is questionable but very probable since we could suspect its activity as regards to the slowing down of the telomere length decrease (110 bp/MPD before crisis, 69 bp/MPD right after crisis, followed by a stabilization of telomere length). This is even more obvious for long telomeres (decrease of 400 bp/MPD before crisis and 58 bp/MPD after crisis). A balance between elongation and telomere decrease could occur in favor of a global decrease of the telomere length and persist until telomeres reach an optimal size where mean TRFs stay stable with slight oscillations (Figure 12).

The link between telomere length and chromosomal instability, in a telomerase activity context, depended upon a complex interaction among the system of telomere length maintenance. The mechanism of end-to-end fusion prevention is not elucidated. Telomere length *per se* is not sufficient to avoid fusions. Telomere binding proteins such as TRF1 or TRF2 could prevent telomerase to bind to telomeres by changing the structure of the telomeres or by protecting chromosome ends from end-to-end fusions. However, we did not see a correlation between telomere length regulation and the expression rate of TRF1 and TRF2. We cannot correlate the expression of telomeric proteins TRF1 and TRF2 with the decrease of chromosomal instability when telomerase activity is detectable and mean telomere lengths shorten. It is not excluded that TRF1 and TRF2 levels could be regulated on a translational level. Therefore other mechanisms could regulate telomere length and chromosomal instability in these cells.

The function of telomerase to maintain telomere integrity is not that simple. Telomerase could be active on each telomere independently thus reducing the heterogeneity of telomere length observed by FISH giving rise to a more homogeneous group of distal telomeres in immortal cells as observed in Figure 8c at passage 55 and Figure 9. Telomerase could protect short telomeres which have reached a 'critical' length, responsible for the chromosomal instability. This was confirmed by the low level of chromosomal instability observed after crisis. The telomere length under which telomerase adds telomeric repeat sequences is difficult to estimate. In terms of mean TRF, the critical length seems different for each cell line, however the heterogeneity of the length of subtelomeric arrays could be involved in these discrepancies. This would imply a large polymorphism between cell lines in these regions.

In conclusion, we have shown that short and long telomeres could present different behaviors. Just after crisis, telomerase could protect specifically the telomeres which have reached a critical size, thus preventing them from forming end-to-end dicentrics, while long telomeres continue to decrease in immortalized human fibroblasts.

Material and methods

Transfection

TP15.5, Fou GB1.6, Peteb PB1.2 and MRC5 3.7 cell lines were established by transfection of normal primary human skin fibroblast cell cultures (from ear, arm, face and lung respectively) with a plasmid containing SV40 sequences (pMK16- SV40 ori-) using the calcium phosphate coprecipitation method (Graham and van der Eb., 1973). After transfection, ring clones emerging from crisis were isolated. Only a subset of these clones had the capacity to proliferate indefinitely. For the cell line TP, transfected at passage 14, out of the 17 ring clones individually isolated and separated, only one clone had the capacity to become immortal, giving rise to TP15.5. For each cell line, the immortal cells analysed grew out from one single ring clone.

Clonality of SV40 cell lines

For the four cell lines analysed, the clonality of SV40 fibroblast populations was monitored by chromosome banding and hybridization of a biotin labeled SV40 sequence probe on metaphase spreads at different passages. The constant viral integration site through passages proved the immortalized cell lines to be clonal early after crisis and later on.

Cell cultures

All cells were grown in minimal essential medium (Gibco) containing 10% fetal calf serum and were incubated at 37°C in a humidified incubator with 5% CO_2. Cells were subcultured when confluent and reseeded for TP15.5 at a split ratio of 1 : 4 from 26 to 46 MPD (passages 3 – 13), 1 : 8 up to 79 MPD (passage 24), 1 : 16 up to 143 MPD (passage 40) and 1 : 32 for further passages. The crisis period occurred around 38 MPD (passage 9) and lasted 2 months for TP15.5. Crisis started at passage 8 and immortalized TP15.5 cells emerged at passage 10. Similar cell culture conditions were performed before and after crisis for the other cell lines.

Cytogenetic studies

Chromosome preparations were performed according to standard techniques (Dutrillaux and Couturier, 1981). Metaphases were analysed in giemsa at each passage, scoring an average on 50 – 100 mitoses. Morphological chromosomal abnormalities were searched as the number of dicentric and ring chromosomes reflect the general instability of the cells. Ten R-banded karyotypes were established every five passages in order to follow specific anomalies corresponding to particular chromosomes.

In situ *hybridization*

Slides underwent two rounds of fixation/rinses separated by a pepsin treatment. After a dehydration step, air-dried slides were hybridized with a probe mixture containing fluorescent-labeled peptide nucleic acid (PNA)$(CCCTAA)_3$. Denaturation of the DNA was followed by hybridization at 25°C for 2 h and washes (Lansdorp *et al*., 1996). Chromosomes were covered with counterstaining DAPI and slides were mounted with anti-fading solution (VectaShield, Biosis, Compiègne).

Image acquisition and processing

After microscopic observations, digital images were recorded with a cooled KAF 1600 CCD 12 bits video camera (Lhesa electronics) driven by Aphelion Software (ADCIS), on a Leica DMRB epifluorescence microscope. A N2.1 (LP 580 nm) filter block (Leica) was used for the visualization of Cy3 and an A (LP 430 nm) filter block (Leica) for DAPI. Image processing was performed under NIH Image 1.61

(http://rsb.info.nih.gov/nih-image/). For each metaphase studied, telomeric fluorescence was quantified after local background substraction. After thresholding, the resulting binary images were used to select double telomeric spots of sister chromatids on each chromosome arm. Area and grey levels of these spots were then measured and exported in Profit 5.0.1 (Quantum Soft, Zurich, Switzerland). Measurement normalization was performed by dividing each spot intensity by the corresponding acquisition time rendering a mean flux directly proportional to the telomere length. Statistical analysis were performed under Statview 4.02 (Abacus Concept, inc.). Ten metaphases of a same slide were analysed under these conditions for each studied passage to obtain telomere fluorescence values.

Similar analysis were performed on interphasic nuclei. Thresholded images underwent morphological operations in order to obtain distinct nuclei borders. Telomeric intensities were normalized by DNA quantity estimated by the corresponding DAPI intensities and corrected with the integration time. Forty-six, 150, 170 and 165 nuclei were analysed respectively for TP, TP15.5 p5, p11 and p55.

Preparation of protein extracts and telomerase activity

Cells (10^6 were washed in ice-cold phosphate-buffered saline and detached from the flasks by incubation with ice-cold PBS-1 mM EDTA for 20 min at 37°C and collected by centrifugation for 5 min at 2000 *g* at 4°C. The supernatant was then treated according to Kim *et al*. (1994). The final pellets were used for DNA analysis. Protein concentration was determined by the Bradford (Bio-Rad) protein assay. Telomerase activity was studied on 2 μl of protein extract using the TRAPeze kit (Appligene, Illkirch) and a protein concentration ranging from 2 ng to 0.1 μg (depending on the cell lines) for the ELISA PCR telomerase kit (Boehringer-Mannheim, Meylan). PCR was performed for 27 or 30 cycles. Products from TRAPeze were resolved by electrophoresis in nondenaturing 12.5% polyacrylamide gels. Gels were exposed with an intensifying screen for 5–24 h.

Analysis of telomeric DNA

DNA was extracted from the final pellets resulting from the protein extraction and purified by phenol/chloroform extractions in order to study telomere length and telomerase activity of the exact same cells. To estimate the length of telomeric repeats, 2 μg of DNA samples were digested with restriction endonucleases *Rsa*I and *Hinf*I, fractionated by 0.5% agarose gel electrophoresis overnight and transferred to nylon membranes by the method of Southern blot, followed by cross-linking with UV light. The filter was hybridized to γ-^{32}P-ATP labeled $(TTAGGG)_4$ telomeric probe. Hybridization was carried out at 42°C for at least 16 h. The filter was then washed with 2 × SSPE- 0.1% SDS and exposed to Amersham film with an intensifying screen for 2–7 days. After removal of the first probe, DNA loading and integrity were checked by rehybridizing the same blot with a $(CAC)_5$ microsatellite probe. Southern blots were performed in triplicates for TP15.5 and in duplicates for the other cell lines in order to calculate mean TRF lengths. Standard deviation values evolved between 1.05×10^{-3} and 0.633 in TP15.5, 0.025 and 0.125 in Peteb PB1.2, 0.02 and 0.125 in MRC5 3.7, 0.53 and 2.03 in Fou GB1.6.

Technique for evaluating telomere length

The autoradiographic film was digitalized with a scanner under Photoshop (Adobe) at 63.5 lines per inch. For each lane, migration profils were then extracted under image (NIH image V1.57). Position of migration standard bands (1 kb ladder, Gibco BRL Life Technologies) were reported on the film prior to digitalization.

Migration distance were expressed in pixels and signal intensity in grey levels. Each profile (signal-distance) was reported into Profit (Quantum Soft) which provided non linear curve fittings and integration facilities.

The first step to calculate mean TRF length was to obtain a migration function giving the length of the DNA fragment at any distance in the gel. We used a four parameter logistic equation for accurate values of DNA (Oerter *et al*., 1990).

$$\text{length distance} = \frac{a \quad d}{1 + \left(\frac{\text{Length}}{c}\right)^{\text{b}}} + d$$

After background substraction from TRF densitometric profiles, the mean TRF length was calculated as

$$\overline{TRF} = \sum_i L_i \frac{S_i}{\sum_i S_i}$$

where L_i is the reciprocal function of the migration function and S_i the densitometric signal.

Bal 31 digestion of telomeres

Three μg of intact DNA was digested with 1,2U of Bal 31 for 2, 5, 7, 10 and 20 min in NaCl 600 mM, $MgCl_2$ 24 mM, $CaCl_2$ 24 mM and Tris pH 8 40 mM. The DNA was subsequently precipitated and digested as for classical TRF analysis.

Northern blot

RNA extractions were performed using TRIzol (Gibco BRL Life Technologies). Fifteen μg of RNAs were charged on a 1% agarose gel in MAE 1X. The electrophoresis lasted 3 h at 100 V with circulating buffer. The transfer on a vacuum-blot was followed by a hybridization with α-^{32}P-dCTP labeled PCR TERC with a random priming kit (Boehringer). TERC probe was obtained by PCR amplification with primers 5′-GCCTTCCACCGTTCATTCTA-3′ and 5′-ATGTGTGAG-CCGAGTCCTG-3′. Probe 28S, labeled with γ^{32}PATP, enabled us to monitor the deposits on the gel in order to quantify TERC.

RT–PCR

cDNA resulted from reverse-transcription of 2 μg RNA treated with DNase and RNasin. 30 cycles of PCR amplification produced a band of 550 bp for GAPDH (internal control) and 35 cycles gave rise to major signals of 421, 636, 264 and 855 bp with TRF1, TRF2, TEP1 and TERT respectively. The experiment was performed in triplicate for each studied cDNA.

GAPDH primers:	5′-ACCACCATGGAGAAGGCTGG-3′
	5′-CTCAGTGTAGCCCAGGATGC-3′
TRF1 primers:	5′-TGTGCGGATGGTAGGGATGC-3′
	5′-GGGCTGATTCCAAGGGTGTA-3′
TRF2 primers:	5′-AGTCAATCGCTGGGTGCTCA-3′
	5′-CCTGGTGCTGGCTGTTTATC-3′
TEP1 primers:	5′-TCAAGCCAAACCTGAATCTGAG-3′
	5′-CCCGAGTGAATCTTTCTACGC-3′
TERT primers:	5′-CCTGCGTTTGGTGGATGATT-3′
	5′-GGCTGCTGGTGTCTGCTCTC-3′

Acknowledgements
We thank M Ricoul, S Gallimant V Debonne, E Grégoire, G Pottier and C Gzanotier for their helpful technical assistance, C Brun for her advice on Bal 31 experiments, J Lebeau for the cell lines establishments, C Desmaze for comments on the manuscript and E Gilson for helpful discussions. This work was supported by CEC.PL 950008, EDF France n° 8703 and ACC-SV 8.

References

Allsopp RC, Vaziri H, Patterson C, Goldstein S, Younglai EV, Futcher AB, Greider CW and Harley CB. (1992). *Proc. Natl. Acad. Sci. USA,* **89,** 10114–10118.

Benn PA. (1976). *Am. J. Hum. Genet.,* **28,** 465–473.

Bilaud T, Brun C, Ancelin K, Koering CE, Laroche T and Gilson E. (1997). *Nature Genet.,* **17,** 236–239.

Blasco M, Rizen M, Greider CW and Hanahan D. (1996). *Nature Genet.,* **12,** 200–204.

Bodnar AG, Ouellette M, Frolkis M, Holt SE, Chiu C-P, Morin GB, Harley CB, Shay JW, Lichtsteiner S and Wright WE. (1998). *Science,* **279,** 349–352.

Broccoli D, Smogorzewska A, Chong L and de Lange T. (1997). *Nature Genet.,* **17,** 231–235.

Counter CM. (1994). *J. Virol.,* **68,** 3410–3414.

Counter CM, Avilion AA, LeFeuvre CE, Stewart NG, Greider CW, Harley CB and Bacchetti S. (1992). *EMBO J.,* **11,** 1921–1929.

Dutrillaux B and Couturier J. (1981). *La pratique de l'analyse chromosomique*. Masson: Paris.

Feng J, Funk WD, Wang SS, Weinrich SL, Avilion AA, Chiu CP, Adams RR, Chang E, Allsopp RC and Yu J, *et al.* (1995). *Science,* **269,** 1236–1241.

Filatov L, Golubovskaya V, Hurt JC, Byrd LL, Phillips JM and Kaufmann WK. (1998). *Oncogene,* **16,** 1825–1838.

Graham FL and van der Eb AJ. (1973). *Virology,* **64,** 456–467.

Greider CW. (1991). *Cell,* **67,** 645–647.

Greider CW and Blackburn EH. (1985). *Cell,* **43,** 405–413.

Greider CW and Blackburn EH. (1987). *Cell,* **51,** 887–898.

Harley CB. (1991). *Mutation Res.,* **256,** 271–282.

Harrington L, Zhou W, McPhail T, Oulton R, Yeung DSK, Mar V, Bass MB and Robinson MO. (1997). *Genes Dev.,* **11,** 3109–3115.

Hayflick L and Moorhead P. (1961). *Exp. Cell. Res.,* **25,** 585–621.

Holt SE, Wright WE and Shay JW. (1996). *Mol. Cell. Biol.,* **16,** 2932–2939.

Jiang XR, Jimenez G, Chang E, Frolkis M, Kusler B, Sage M, Beeche M, Bodnar AG, Wahl GM, Tlsty TD and Chiu CP. (1999). *Nature Genet.,* **21,** 111–114.

Jones CJ, Soley A, Skinner JW, Gupta J, Haughton MF, Wyllie FS, Schlumberger M, Bacchetti S and Wynford-Thomas D. (1998). *Exp. Cell. Res.,* **240,** 333–339.

Kim NW, Piatyszek MA, Prowse KR, Harley CB, West WD, Ho PL, Coviello GM, Wright WE, Weinrich SL and Shay JW. (1994). *Science,* **266,** 2011–2014.

Klingelhutz AJ, Barber SA, Smith PP, Dyer K and McDougall JK. (1994). *Mol. Cell. Biol.,* **14,** 961–969.

Lansdorp PM, Verwoerd NP, van de Rijke FM, Dragowska V, Little M-T, Dirks RW, Raap AK and Tanke HJ. (1996). *Hum. Mol. Genet.,* **5,** 685–691.

Lingner J, Cooper JP and Cech TR. (1995). *Science,* **269,** 1533–1534.

McClintock B. (1939). *Proc. Natl. Acad. Sci. USA,* **25,** 405–416.

Meyerson M, Counter CM, Eaton EN, Ellisen LW, Steiner P, Dickinson Caddle S, Ziaugra L, Beijersbergen RL, Davidoff MJ, Liu Q, Bacchetti S, Haber DA and Weinberg RA. (1997). *Cell,* **90,** 785–795.

Morales CP, Holt SE, Ouellette M, Kaur KJ, Yan Y, Wilson KS, White MA, Wright WE and Shay JW. (1999). *Nature Genet.,* **21,** 115–118.

Nakayama J-i, Tahara H, Tahara E, Saito M, Ito K, Nakamura H, Nakanishi T, Tahara E, Ide T and Ishikawa F. (1998). *Nature Genet.,* **18,** 65–68.

Oerter KE, Munson PJ, McBride WO and Rodbard D. (1990). *Anal. Biochem.,* **189,** 235–243.

Olovnikov A. (1973). *J. Theor. Biol.,* **41,** 181–190.

Rhyu MS. (1995). *J. Natl. Cancer Inst.,* **87,** 884–894.

Rubin H. (1998). *Nat. Biotech.,* **16,** 396–397.

Sandell LL and Zakian VA. (1993). *Cell,* **75,** 729–739.

Shay JW, Pereira-Smith OM and Wright WE. (1991). *Exp. Cell. Res.,* **196,** 33–39.

Shen M, Haggblom C, Vogt M, Hunter T and Lu KP. (1997). *Proc. Natl. Acad. Sci. USA,* **94,** 13618–13623.

Sprung CN, Sabatier L and Murnane JP. (1998). *Exp. Cell Res.,* in press.

Tommerup H, Dousmanis A and de Lange T. (1994). *Mol. Cell. Biol.,* **14,** 5777–5785.

van Steensel B and de Lange T. (1997). *Nature,* **385,** 740–743.

van Steensel B, Smogorzewska A and de Lange T. (1998). *Cell,* **92,** 401–413.

Wan TSK, Martens UM, Poon SSS, Tsao S-W, Chan LC and Landsdorp PM. (1999). *Genes Chrom. Cancer,* **24,** 83–86.

Watson JD. (1972). *Nature,* **239,** 197–201.

Wright JH and Shay JW. (1992). *Esp. Geron,* **27,** 383–389.

Wright WE, Pereira-Smith OM and Shay JW. (1989). *Mol. Cell. Biol.,* **9,** 3088–3092.